Kinematic Analysis of the Effective Reeling Interval of a Rapeseed Combine Harvester Reel at Different Reel Indices

Yiming Zhang[a]

School of Agricultural Engineering, Jiangsu University, Zhenjiang 212013, China

[a]2222516031@stmail.ujs.edu.cn

Abstract

To clarify the interaction between reel tines and the rapeseed canopy under different reel-index conditions, a conventional fixed-diameter reel was investigated. A kinematic model of the tine endpoint was established by coupling the forward motion of the combine harvester with the rotary motion of the reel, and the tine trajectories and horizontal motion characteristics at different reel indices were analyzed. The effective reeling interval was then defined by combining the spatial distribution of the rapeseed canopy with two criteria: the tine endpoint had to lie within the effective canopy-height range and possess a backward horizontal velocity component. Effective action angle, effective action time, and effective horizontal action range were used to characterize reeling performance. The results showed that the reel index markedly affected both the tine trajectory and the effective reeling interval. When the reel index exceeded 1, a backward-motion segment occurred in the tine trajectory. As the reel index increased, the effective action angle and horizontal action range changed systematically, whereas the effective action time was jointly governed by the action angle and reel angular velocity. The proposed method provides a theoretical basis for matching the operating parameters of conventional reels used on rapeseed combine harvesters.

Keywords

Rapeseed; Combine Harvester; Reel; Reel Index; Motion Trajectory; Effective Reeling Interval.

1. Introduction

The reel is a key working component of a combine-harvester header. Its principal functions are to support and guide the crop and to convey the cut plants toward the rear of the header. Rapeseed plants are tall, highly branched, and prone to pod shattering. Consequently, reel position and rotational speed, together with their coordination with harvester forward speed, directly affect crop conveyance at the header and seed loss [4,7-8].

The kinematic characteristics of harvesting reels have been extensively investigated. Oduori et al. [1] developed a kinematic model for the tines of a conventional reel and analyzed the effects of the reel index on trajectory shape and crop-engagement timing. Yang et al. [2] analyzed the crop-engaging trajectory of a reel used on a rapeseed combine harvester. Zhang et al. [3] developed a double-crank planar five-bar reel and investigated the motion law of its reel fingers. These studies provide a foundation for reel-trajectory design and parameter matching; however, the coupling between a conventional tine trajectory and the spatial extent of the rapeseed canopy has not yet been quantitatively described.

Therefore, a conventional fixed-diameter reel was investigated in this study. A kinematic model of the tine endpoint was established, with the reel index treated as the principal variable. The effective reeling interval was defined by combining the rapeseed canopy-height range with the horizontal direction of tine motion. Changes in effective action angle, effective action time, and horizontal action range were then analyzed at different reel indices. The results provide a theoretical reference for coordinating reel speed, installation position, and harvester forward speed in rapeseed harvesting.

2. Kinematic Model of a Conventional Reel

2.1 Reel Motion Model

A conventional reel mainly consists of a reel shaft, end discs, spokes, tine bars, and tines. Its motion is generally analyzed as the superposition of machine translation and reel rotation [1,9]. During harvesting, the combine harvester travels forward at a constant speed while the reel rotates uniformly about its own axis. Thus, the absolute motion of a tine endpoint is jointly determined by the forward motion of the machine and the rotary motion of the reel. To simplify the analysis, the harvester forward speed and reel angular velocity were assumed to remain constant, the reel working radius was assumed to be invariant, and the effects of ground unevenness, machine vibration, and the reaction of rapeseed plants on tine motion were neglected.

To illustrate the relationships among the motion parameters, the fixed coordinate system xOy shown in Fig. 1 was established. The positive x-axis coincides with the forward direction of the combine harvester, and the y-axis is vertically upward. Let R denote the reel working radius, H the height of the reel center above the ground, v_m the harvester forward speed, ω the reel angular velocity, and P the tine endpoint. The reel angle θ was measured from the position at which the tine is at the lowest point.

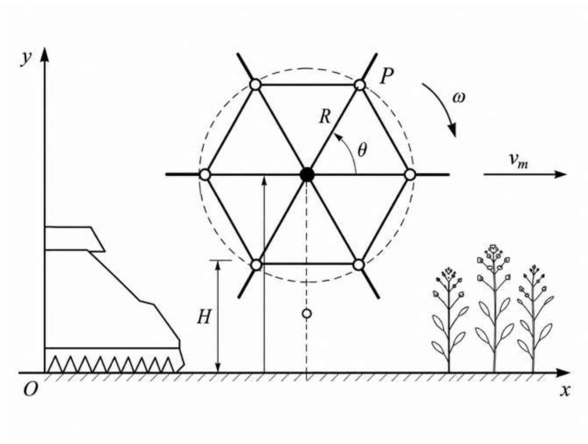

Fig. 1 Kinematic model of a conventional reel tine

According to the motion relationships shown in Fig. 1, the reel angle is related to time by

$$\theta=\omega t \tag{1}$$

where θ is the reel angle, rad; ω is the reel angular velocity, rad/s; and t is time, s.

2.2 Motion Trajectory of the Tine Endpoint

In the fixed coordinate system, the reel center translates uniformly along the x-axis with the combine harvester, and its horizontal displacement is $v_m t$. The tine endpoint moves in a circle of radius R relative to the reel center. Therefore, the equations of motion of tine endpoint P are

$$x=v_m t-R\sin\theta \tag{2}$$

ISSN: 2414-1895 DOI: 10.6919/ICJE.202609_12(9).0003

$$y=H-R\cos\theta \tag{3}$$

where x is the horizontal displacement of the tine endpoint, m; y is the height of the tine endpoint above the ground, m; R is the reel working radius, m; H is the height of the reel center above the ground, m; and v_m is the harvester forward speed, m/s.

Differentiating Eqs. (2) and (3) with respect to time gives the horizontal and vertical velocity components of the tine endpoint, respectively:

$$v_x=v_m-R\omega\cos\theta \tag{4}$$

$$v_\gamma=R\omega\sin\theta \tag{5}$$

$$v_p=\sqrt{(v_x^2+v_\gamma^2)} \tag{6}$$

where v_x is the horizontal velocity of the tine endpoint, m/s; v_γ is its vertical velocity, m/s; and v_p is its absolute velocity, m/s.

Equations (2)-(6) show that the reel working radius, harvester forward speed, and reel angular velocity jointly determine the trajectory and velocity characteristics of the tine endpoint. In particular, matching the reel peripheral speed to the harvester forward speed is a major factor governing tine-trajectory shape.

2.3 Reel Index and Backward-Motion Interval

The reel index is a commonly used dimensionless parameter that characterizes the relationship between reel peripheral motion and machine forward motion. It determines whether the tine trajectory forms a loop that facilitates crop engagement and rearward conveying [1-2,5]. For the subsequent derivation, the reel index λ is defined as

$$\lambda=\omega R/v_m \tag{7}$$

where λ is the reel index.

Substitution of Eq. (7) into Eq. (4) gives

$$v_x=v_m(1-\lambda\cos\theta) \tag{8}$$

When the horizontal tine velocity $v_x<0$, the tine has a horizontal velocity component opposite to the forward direction of the combine harvester relative to the ground and can therefore convey the crop toward the rear of the header. According to Eq. (8), the criterion for backward tine motion can be simplified to

$$\lambda\cos\theta>1 \tag{9}$$

Equation (9) shows that when $\lambda\leq1$, no backward horizontal motion occurs near the lowest tine position. When $\lambda>1$, backward motion occurs over a finite angular interval on both sides of the lowest position. The critical angle is

ISSN: 2414-1895 DOI: 10.6919/ICJE.202609_12(9).0003

$$\theta_0=\arccos(1/\lambda) \tag{10}$$

where θ_0 is the critical angle for backward tine motion, rad.

Therefore, the theoretical angular range of backward tine motion is

$$-\theta_0<\theta<\theta_0 \tag{11}$$

As the reel index increases, the critical angle θ_0 increases and the angular range over which the tine has a backward horizontal velocity component gradually expands. Typical trajectories calculated from Eqs. (2), (3), and (7) may be arranged as shown in Fig. 2 to compare loop shape, lowest-point position, and the backward-motion segment at different reel indices.

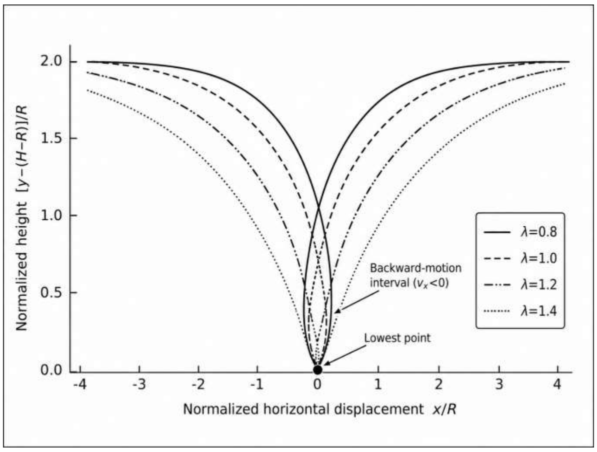

Fig. 2 Theoretical trajectories of the tine endpoint at different reel indices

3. Determination of the Effective Reeling Interval under Rapeseed-Canopy Constraints

3.1 Spatial Range of the Rapeseed Canopy

Rapeseed plants are highly branched, and their canopy and pod layers exhibit distinct vertical distributions. Plant morphology also varies with cultivar and harvest condition [5,8,10]. A tine can effectively support and convey plants only when it enters the rapeseed canopy and simultaneously develops a rearward velocity component. Therefore, the upper and lower boundaries of the rapeseed canopy were used as spatial constraints on the tine trajectory.

Based on field investigation of the rapeseed canopy, the effective canopy was mainly distributed within a height range of 1.35–1.60 m above the ground. Accordingly, the lower and upper boundaries of the effective canopy were set as h1=1.35 m and h2=1.60 m, respectively.

Based on field investigation of the rapeseed canopy, the effective canopy was mainly distributed within a height range of 1.35–1.60 m above the ground. Accordingly, the lower and upper boundaries of the effective canopy were set as h1=1.35 m and h2=1.60 m, respectively.

Let h_1 and h_2 denote the heights of the lower and upper boundaries of the effective rapeseed canopy above the ground, respectively, with $h_1<h_2$. A tine endpoint within the effective canopy range must satisfy

$$h_1\le y\le h_2 \tag{12}$$

ISSN: 2414-1895 DOI: 10.6919/ICJE.202609_12(9).0003

Substituting Eq. (3) into Eq. (12) and rearranging converts the canopy-height constraint into an angular constraint:

$$(H-h_2)/R \leq \cos\theta \leq (H-h_1)/R \tag{13}$$

The reel angles corresponding to the intersections of the tine trajectory with the lower and upper canopy boundaries are defined as

$$\theta_1=\arccos[(H-h_1)/R] \tag{14}$$

$$\theta_2=\arccos[(H-h_2)/R] \tag{15}$$

where h_1 is the height of the lower boundary of the effective rapeseed canopy above the ground, m; h_2 is the height of the upper boundary, m; θ_1 is the reel angle when the tine reaches the lower canopy boundary, rad; and θ_2 is the reel angle when the tine reaches the upper canopy boundary, rad.

When the canopy boundaries intersect the circular tine path, $\theta_1<\theta_2$. Considering the process in which the tine descends through the front of the reel and enters the uncut rapeseed canopy, the canopy-constrained angular range is

$$-\theta_2 \leq \theta \leq -\theta_1 \tag{16}$$

This study focuses on the descending portion at the front of the reel. The ascending portion at the rear mainly guides and conveys cut plants and is therefore excluded from the effective reeling interval of the uncut canopy. The upper and lower canopy boundaries, the descending tine trajectory at the front of the reel, and the corresponding angular relationships are illustrated in Fig. 3.

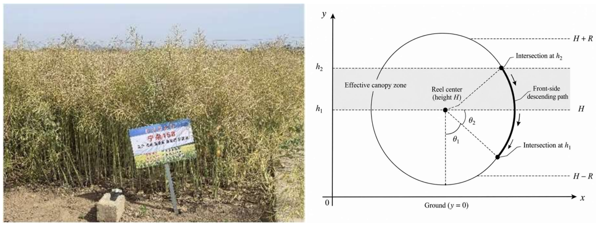

(a) (b)

Fig.3 Field investigation of the rapeseed canopy and definition of the canopy-constrained tine motion interval

(a) Field measurement of rapeseed canopy height

(b) Definition of canopy-constrained tine motion interval

3.2 Determination of the Effective Reeling Interval

Previous studies have shown that reel speed, vertical position, and finger-motion mode alter tine-plant contact and header performance [3-4,6]. Entry of a tine into the rapeseed canopy only indicates the possibility of spatial contact. If its horizontal motion is in the same direction as harvester travel, the tine tends to push the plants forward and cannot effectively convey them toward the rear of the header. The effective reeling interval must therefore satisfy both the canopy spatial constraint and the backward-motion constraint.

ISSN: 2414-1895 DOI: 10.6919/ICJE.202609_12(9).0003

The canopy-constrained range and backward-motion range have already been derived. Taking the intersection of the canopy angular range in Eq. (16) and the backward-motion range in Eq. (11), define

$$\theta_e=\min(\theta_2,\theta_0) \tag{17}$$

where θ_e is the smaller of the reel angle at the upper canopy boundary and the critical angle for backward motion, rad. The effective reeling interval on the front side of the reel is then

$$-\theta_e\le\theta\le-\theta_1 \tag{18}$$

The condition for the existence of an effective reeling interval is

$$\lambda>1,\theta_e>\theta_1 \tag{19}$$

When $\lambda\le1$, the required backward-motion segment cannot form. When $\lambda>1$ but $\theta_0\le\theta_1$, backward motion occurs below the prescribed effective canopy-height range, so no effective reeling interval is formed. The complete determination procedure is summarized in Fig. 4.

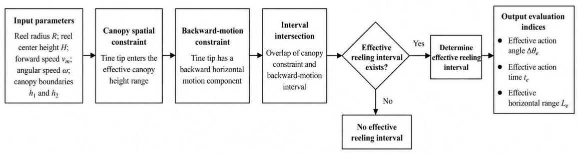

Fig.4 Determination and evaluation procedure of effective reeling interval

3.3 Evaluation Indices for Effective Reeling Characteristics

To quantitatively evaluate tine action on the rapeseed canopy at different reel indices, the effective action angle, effective action time, and effective horizontal action range were selected as evaluation indices.

3.3.1 Effective Action Angle

The effective action angle is the angle through which the tine rotates within the effective reeling interval and can be expressed as

$$\Delta\theta_e=\theta_e-\theta_1 \tag{20}$$

where $\Delta\theta_e$ is the effective tine-action angle, rad. When the condition in Eq. (19) is not satisfied, $\Delta\theta_e=0$. This index represents the angular range that simultaneously satisfies the canopy-height and backward-motion requirements.

3.3.2 Effective Action Time

When the reel rotates at a constant angular velocity, the effective action time is jointly determined by the effective action angle and the reel angular velocity. Using Eq. (7), it can be written directly as

$$t_e=R\Delta\theta_e/(\lambda v_m) \quad (21)$$

where t_e is the time required for a single tine to pass through the effective reeling interval, s. The effective action time depends not only on the effective action angle but also on the reel index and harvester forward speed.

3.3.3 Effective Horizontal Action Range

Substituting $t=\theta/\omega$ and Eq. (7) into Eq. (2), the horizontal coordinate of the tine endpoint can be expressed as

$$x=R(\theta/\lambda-\sin\theta) \quad (22)$$

Within the effective reeling interval, the horizontal tine velocity remains negative and the horizontal coordinate decreases as the reel angle increases. The difference between the horizontal coordinates at the start and end of the interval gives

$$L_e=R[\sin\theta_e-\sin\theta_1-(\theta_e-\theta_1)/\lambda] \quad (23)$$

where L_e is the horizontal projection length of the effective tine trajectory, m. The effective horizontal action range represents the distance over which the tine moves toward the rear of the header while within the rapeseed canopy. By varying the reel index λ in Eqs. (20), (21), and (23), the changes in effective action angle, effective action time, and effective horizontal action range can be obtained.

4. Conclusion

(1) A displacement, velocity, and trajectory model of the tine endpoint of a conventional reel was established by superimposing uniform harvester translation and uniform reel rotation. The analysis showed that the reel index λ determines whether the tine develops a horizontal motion segment directed backward relative to the ground. A reel index of $\lambda>1$ is necessary for this segment to occur, and the critical angle θ_0 increases with λ.

(2) A method for determining the effective reeling interval was developed by coupling the effective rapeseed canopy-height range with the backward-motion condition of the tine. The interval is the intersection of the canopy spatial constraint and the motion-direction constraint. Its existence and extent are jointly determined by λ, R, H, v_m, and the lower and upper canopy boundaries h_1 and h_2, and cannot be evaluated from the reel index alone.

(3) Three evaluation indices - effective action angle $\Delta\theta_e$, effective action time t_e, and effective horizontal action range L_e - were proposed to compare the theoretical interaction between a tine and the rapeseed canopy at different reel indices. The model provides an analytical framework for coordinating reel speed, installation height, and harvester forward speed. Further work should combine measured canopy parameters with field tests of header loss to determine suitable parameter ranges for specific machine models.

References

[1] Oduori, M. F., Mbuya, T. O., Sakai, J., & et al. (2012). Kinematics of the tined combine harvester reel. *Agricultural Engineering International: CIGR Journal*, 14(3), 53–60.

[2] Yang, Y., Li, Y. M., & Qing, Y. R. (2020). Analysis and experiment of the crop-engaging trajectory of a rapeseed combine-harvester reel. *Journal of Agricultural Mechanization Research*, 42(10), 189–194. (in Chinese)

ISSN: 2414-1895 DOI: 10.6919/ICJE.202609_12(9).0003

[3] Zhang, M., Jin, M., Wang, G., & et al. (2022). Design and experiment of a double-crank planar five-bar reel for a rapeseed windrower. *Transactions of the Chinese Society for Agricultural Machinery*, 53(1), 115–122. (in Chinese)

[4] Wu, W. J., & Wu, C. Y. (2018). Optimization of header parameters for a rapeseed combine harvester. *Journal of Zhejiang University (Agriculture and Life Sciences)*, 44(4), 481–489. (in Chinese)

[5] Qing, Y. R., Li, Y. M., Yang, Y., & et al. (2021). Development and experiments on reel with improved tine trajectory for harvesting oilseed rape. *Biosystems Engineering*, 206, 19–31.

[6] Li, H. T., Wu, C. Y., Mu, S. L., & et al. (2020). Formation mechanism of the laying angle of a vertical rapeseed windrower based on ANSYS-ADAMS. *Transactions of the Chinese Society of Agricultural Engineering*, 36(14), 96–105. (in Chinese)

[7] Hobson, R. N., & Bruce, D. M. (2002). Seed loss when cutting a standing crop of oilseed rape with two types of combine harvester header. *Biosystems Engineering*, 81(3), 281–286.

[8] Qing, Y. R., Li, Y. M., Xu, L. Z., & et al. (2021). Screen oilseed rape (Brassica napus) suitable for low-loss mechanized harvesting. *Agriculture*, 11(6), 504.

[9] Li, Y. M. (2014). *Design and analysis of grain combine harvesters*. China Machine Press. (in Chinese)

[10] Wu, C. Y. (2017). *Mechanized harvesting technology for rapeseed*. Jiangsu University Press. (in Chinese)